A co-powered Concentrated Solar Power concept for small size combined Heat and Power

Domenico Borello, Alessadnro Corsini , Franco Rispoli and Eileen Tortora

Dipartimento di Meccanica e Aeronautica, Sapienza Università di Roma, Roma, Italy

domenico.borello@uniroma1.it
alessandro.corsini@uniroma1.it
franco.rispoli@uniroma1.it
eileen.tortora@uniroma1.it ***(CA)***

Abstract:

The present work investigates both end-user thermal and electric load matching behaviour of an advanced small scale combined heat and power Rankine cycle plant. The power plant principally consists of a concentrated solar power field and a biomass furnace to produce steam in a Rankine cycle, obtaining electric and thermal energy. A hotel was selected as the end user due to its high thermal to electric consumption ratio. The power plant design and its operation was modelled and investigated, using climate data referred to the latitude of Rome, by adopting a transient simulations with a hourly distribution..The study of the load matching of the proposed renewable power technology and the final user has been carried out by comparing two different load tracking scenarios, i.e. the thermal and the electric demands. As a result, the system power output follows fairly well the given load curves, supplying, on a selected winter day, about 50 GJ/d of thermal energy and the 6 GJ/d of electric energy, with reduced energy dumps when matching the load. Furthermore, for the same winter day, the system allows the reduction of about 4·103 kgCO_2 of greenhouse gas emissions.

Keywords:

Biomass ,Cogeneration, Concentrated Solar Power, Load Matching, Rankine Cycle, Transient Simulation.

1. Introduction

In recent years the use of Combined Heat and Power (CHP) was commonly considered to supply energy to end users in the service or residential sectors. The basic argument in favour of CHP is the possibility to obtain electric and thermal energy in situ, improving the power generation efficiency and reducing the losses usually related to the energy distribution [1, 2]. It is worth noting that among the existing CHP plants, only some exceptions are based the exploitation of different fuels from natural gas, i.e. small-scale power plants based on biomass derived fuel exploitation, like wood or biogas [3, 4].

In most applications, the main factor which determines the economic viability of CHP schemes is the high utilisation of the heat and electric energy, which are produced simultaneously. Most of the literature indicates that the CHP plant needs to be fully utilised providing heat and power for a minimum duty of 4,500 h per annum to gain its breakeven point [5].

When designing renewable energy based CHP technologies, in a distributed generation concept, one of the key factors is the capability of tracking the time-dependent end-user load. Renewable Energy Sources (RES), intermittent by nature, produce inconsistently and somewhat unpredictably power outputs uncorrelated with the end user power demands, typically variable according to predictable daily load profiles. As a consequence of this mismatch the available RES energy may not meet the energy demand, resulting in deficit and surplus energy situations.

Several solutions have been proposed to attenuate the RES-user matching inconsistency. The conventional remedial strategy is to plug the supply gap providing alternative capacity, known as spinning reserve [6]. Among the solutions devoted to RES electric grid integration, it is worth mentioning the use of high capacity energy storage to save the produced energy surplus and

postponing the energy surplus delivery [7, 8], or combining renewable energy sources with complementary intermittencies [9].

In this respect, the present study investigates a CHP scheme combining a parabolic trough field for concentrated solar power (CSP), a thermal energy storage and a biomass furnace as complementary source. It is worth noting that the biomass source is a *sui generis* RES, in fact its storage simplicity permits to customize the power production management, exactly like the fossil fuel sources.

Concerning the parabolic trough field, that device was selected for its high worldwide development among the CSP systems [10]. Nonetheless, an important aspect of these plants is the size, which, is usually large. In fact solar trough plants are characterised by multi-MW sizes, which range up to about 50 MW_{el} for parabolic trough systems. Also the biomass power plants are usually rated in the range 5–100 MW. Even so, while CSP plants size is still growing [11, 12], in the biomass field there are several applications on small-scale biomass power plants [13, 14].

The aim to exploit CSP technology and limit the plant footprint led to the design of a small scale plant, recently presented in [15, 16], composed by a 2,580 m2 parabolic trough field, a thermal energy storage system (TES) and a 1,163 kW biomass furnace to face the solar source fluctuations. A heat transfer fluid (HTF), i.e. diatermic oil, is heated by the parabolic through field and biomass furnace and subsequently it is sent to a heat recovery steam generator where it produces low enthalpy saturated steam that is sent to a 130 kW reciprocating steam engine for the electric energy production. Moreover, the RC economizer is fed by the exhaust gases derived from the biomass combustion. A heat recovery for thermal energy production is obtained, using hot water as heat carrier, in a back-pressure scheme at 134 °C and 300 kPa.

The investigations on the proposed RES-based small-scale CHP Rankine cycle plant, when matched to a typical hotelier end-user were carried out by transient model simulations. The selection of a hotel as end-user was made for its high heat/electricity consumption ratio. The system matching behaviour is analyzed for both thermal and electric load tracking with the aim to demonstrate its capability to meet the end-users energy request on a 24 hour period in a winter day as more challenging for the solar field performance.

The transient model and the simulations were performed in the TRNSYS environment [17] supported by the in-house made types of the biomass furnace and reciprocating steam engine and the STEC component model library [18]. The software TRNSYS was selected as it is a well-known instrument to model complex energy systems, as demonstrated by several studies appeared in the open literature which mostly deal on RES applications in a few fields like small-islands stand alone power systems [8, 19], or, more related to the present paper, on CSP field simulations [20], TES behaviour in solar trough plants [21] and matching to a hospital end-user [16].

2. Combined solar-biomass plant and model description

2.1. Component and system description

The proposed CHP concept, Figure 1, concerns of a solar-biomass Rankine cycle system. The basic equipment of the power block consists of 1,200 kW solar trough field, 360 kW thermal energy storage (TES) and 1,163 kW biomass furnace to feed the heat transfer fluid (HTF) loop and the related RC.

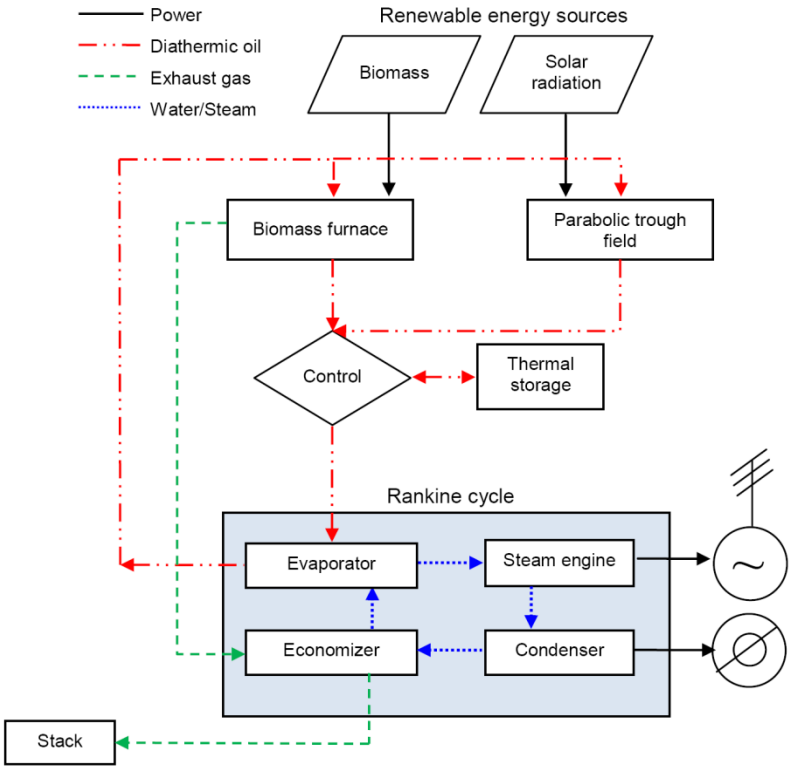

Figure 1. Plant flow chart.

Table 1. Main components description and nominal size.

Component description	Size
Solar parabolic trough field	2,580 m^2, 1,200 kW_{th}
TES	360 kW_{th}
Biomass furnace	1,163 kW_{th}
Reciprocating steam engine	130 kW_{el}
Condenser	1,240 kW_{th}
Diathermic oil circuit	
Maximum/minimum temperature	300/240 °C
Maximum/minimum specific heat	2.36/ 2.19 kJ/kg K
Operating pressure	800 kPa
Water/Steam circuit	
Maximum/minimum pressure	2,800/300 kPa
Maximum/minimum temperature	230/134 °C
Water/steam mass flow rate	0.51 kg/s
Electric power	130 kW
Thermal power	1,100 kW

The HTF circuit supplies the thermal energy to the RC for the production of saturated steam to be expanded in a 130 kW reciprocating steam engine fitted with an electric generator. According to a bottomer CHP configuration, the expanded steam is condensed producing a thermal power output available at a constant temperature of 80 °C, i.e. the temperature demand of typical district heating networks. It is worth noting that the biomass furnace is constantly on duty at a minimum power that is the 35% of its maximum power (i.e. 407 kWth), in order to ease its complementary source role avoiding power output deficits and/or furnace start-up problems related to the Direct Normal Insulation (DNI) sudden variations.

The main components and system thermodynamic parameters, subdivided in diathermic oil and water/steam circuit, are described in Table 1. Additional details concerning the power system components could be found in [15].

The heat exchanges graph is shown in Figure 2. The exhaust gas, diathermic oil and water-steam fluids are represented relating the reached temperatures with the Rankine cycle exchanged power rate. In particular for the exhaust gas two lines are plotted, one (Gas-35%) for the design condition with the biomass furnace working at 35% duty rate, and one (Gas-100%) for the fully biomass duty condition during the solar contribution lacks. The two extreme gas lines detect the range of the solar contribution to the heat exchanges and to the rate of power supply to the Rankine cycle, and thus the biomass energy contribution. IO FAREI UNO ZOOM DELLA ZONA DEL PINCH POINT PER MOSTRARE QUANTO è LA DIFFERENZA DI TEMPERATURA TRA OLIO E VAPORE. MA ABBIAMO CONSIDERATO UNA LAMINAZIONE PER PORTARE IL FLUIDO NEL SURRISCALDATO O ESPANDIAMO SEMPRE NEL SATURO?

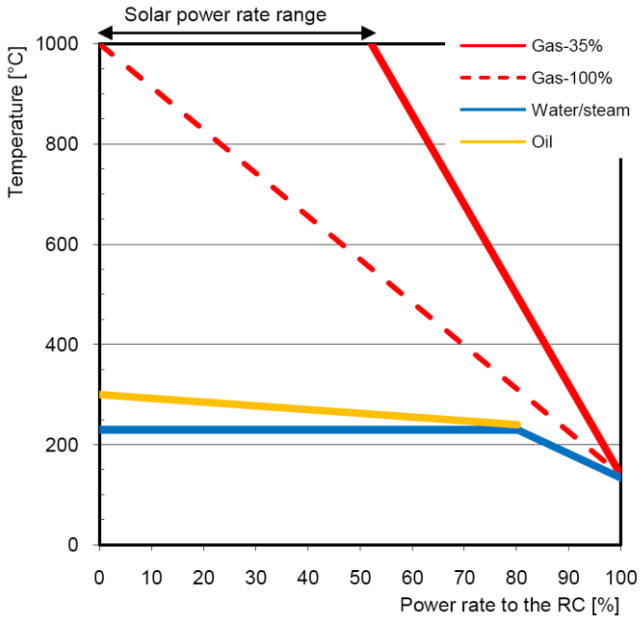

Figure 2. Heat exchanges graph.

2.2. RC transient model description

In order to evaluate the time-dependent behaviour and the performance of the proposed system a transient model was developed in the TRNSYS framework [17] integrated with the STEC library [18]. The RC transient model also includes in-house made types for the biomass furnace and for the reciprocating steam engine [15]. The model subsets and their linkages are described by the flow diagram in Figure 3. The present solar-biomass CHP plant is broadly based on a configuration recently investigated and assessed [15]. HANJALIC MI HA FATTO VEDERE CHE C'E'IN ATTO UNA VERA E PROPRIA CACCIA AL PLAGIO. ATTENZIONE A NON LASCIARE FIGURE INALTERATE OPPURE INDICHIAMO CHIARAMENTE LA CITAZIONE! RIFORMULIAMO SEMPRE LE FRASI!

The base-line model has been implemented by a control logic targeted to the tracking of different loads, namely heat or power demands. The development of the load tracking strategy has been based on the definition of algebraic correlations between the HTF flow rate (1), directly related to the RES power input, and the system thermal power output (P_{th}) or the system electric output (P_{el}), respectively. The HTF flow rate was selected as the reference parameter because it governs the actual power outputs according to the instantaneous renewable energy availability. A sensitivity analysis, was carried out on the power system configuration by varying $\dot{m}_F$ and recording P_{el} and P_{th}

values. Figure 4 shows the values obtained with the sensitivity analysis (grey lines) and the corresponding trendlines (black lines) and equations. The HTF control equations, accordingly derived, read as

$\dot{m}_F = 2 \cdot 10^{-6} \cdot P_{th}^{3.289}$,

$\dot{m}_F = 3.6 \cdot 10^{-2} \cdot P_{el}^{2.713}$.

The control logic was implemented, Figure 3, in order to match the requested HTF flow rate target ($\dot{m}_{F,d}$) at each time-step with the actual power demand according to the adopted load tracking law. Hence, the HTF flow rate target tracks the load evolution following a two-level control strategy, respectively driving the solar section and the whole system. In particular, the solar section control verifies the state of charge of the TES, giving priority to the storage charging in case of emptiness ($\dot{m}_{F,TESc}$). The flow rate not needed to charge the TES can be can be directly supplied to the Rankine cycle. The second control acquires the load data ($\dot{m}_{F,d}$) and compares the HTF flow rate target with the actual HTF flow rate achievable from the available solar field and the minimum biomass furnace rate ($\dot{m}_{F,bmin}$) at each time step, giving rise to three possible situations:

1. direct CSP contribution surplus, the exceeding HTF flow rate will be dumped;
2. direct CSP contribution deficit, the missing heat flux will be first requested to the TES (flow rate $\dot{m}_{F,TESd}$); and
3. in case of insufficient flux from the solar section (flow rate $\dot{m}_{F,s}$) and minimum biomass contributions, an additional heat flux is requested to the biomass furnace (flow rate $\dot{m}_{F,b+}$).

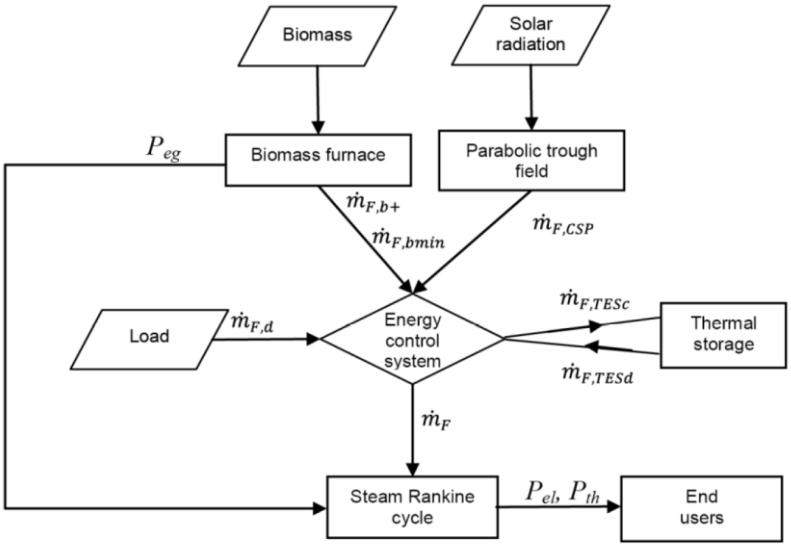

Figure 3. Energy conversion system flow diagram.

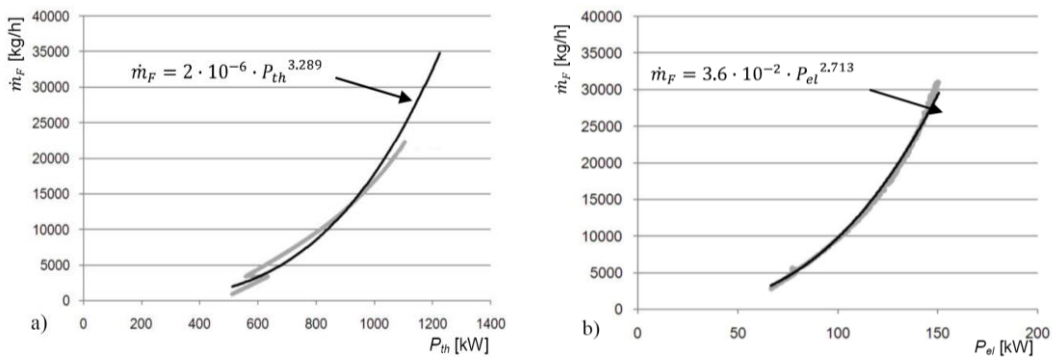

Figure 4. Thermal a) and electric b) output control equations.

3. End user description

3.1. End-user load profile

The behaviour of the proposed RES-based small-scale CHP Rankine cycle plant is investigated in the matching of load curve of a typical hotelier end-user during a 24 hour time period. The hotel was chosen, among tertiary sector end-users, for its high annual heat/electricity consumption ratio. The end-user characteristics are summarized, in Table 2. The energy data gives a heat/electric consumption ratio higher than five, Table 2 [23], which is typical of European hotelier end-user figure, in contrast to the standard North-American hotel energy profile [24]. Furthermore, in order to take into account the cooling load also, it is worthy referring to the equivalent thermal load (obtained by the addition of the actual thermal load and the thermal load resulting if fulfilling the cooling load with a absorption chiller) with a 0,7 COP. In this case the heat/electric rises to a value of 7.44. The cooling load takes place only in the months from June to September, with a constant distribution of about 600 GJ/month.

Table 2. End users characteristics [23].

	Hotel
Volume [m^3]	43˙000
Number of sleeping accommodations	350
Heat load [GJ/y]	8˙640
Electric load [GJ/y]	1˙656
Cooling load [GJ/y]	2˙580
Equivalent thermal load	12˙326
Heat/electric consumption ratio [GJ_{th}/GJ_{el}]	5,23
Equivalent heat/electric consumption ratio [GJ_{th}/GJ_{el}]	7.44

Figure 5 shows the monthly distribution of the electric and equivalent thermal load for the selected end-user; the average daily energy demand (dot sign) is represented in relationship with the daily average power demand (x sign) and the power demand excursion (bar). It is evident that the electric energy request has an almost constant behaviour with average daily energy demand always below 200 GJ/day. Whereas the thermal monthly profile has a seasonal connotation which entails a thermal load range from 250 GJ on the summer period to 1,370 GJ on the winter one. It is worth noting that generally the average power demand is positioned on the lower part of the power demand excursion bars, indicating that the energy demand is composed by frequent low power demand values and rare high power values. This behaviour is highlighted in the summer equivalent thermal load curves (from June to September) of both the end users, when high peaks of cooling energy are requested during the day.

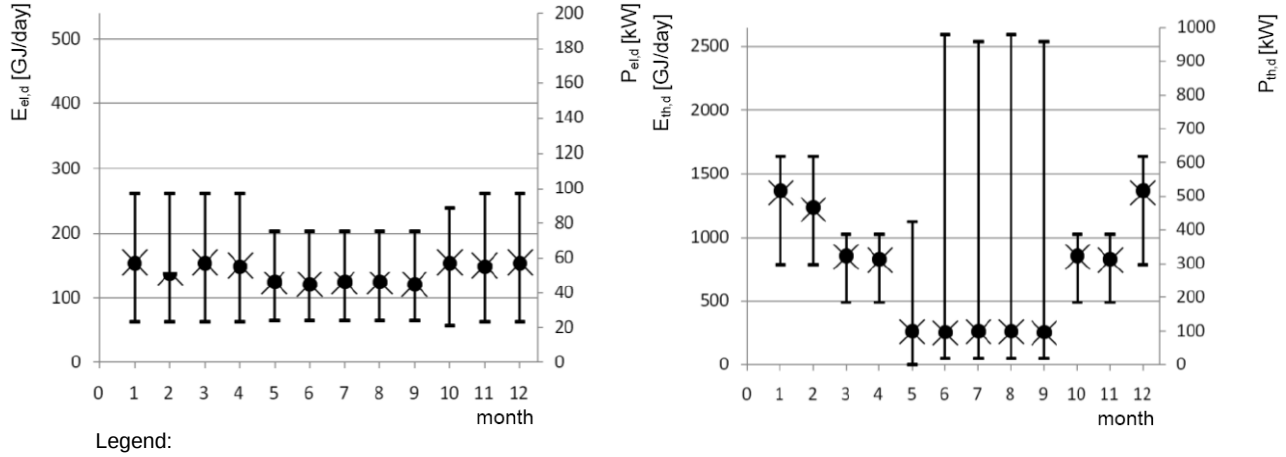

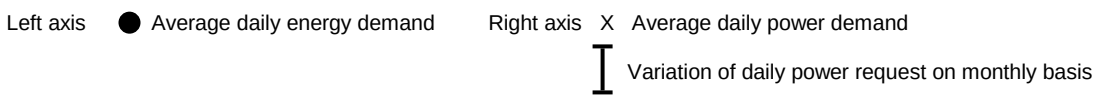

Figure 5. Hotel monthly electric and thermal load yearly behaviour.

3.2. RES data input

The RES input data are available on a hourly distribution over a year period. The direct normal insulation data [25], are referred to Rome's latitude, i.e. 41°54'39"24 N, as indicative of a central Italian location DNI data show a maximum value in the month of July, with 733.68 MJ/m^2 and a minimum value of 253.04 MJ/m^2 in December, with an annual cumulative irradiation of 5,760 MJ/m^2. For what concerns the solar radiation data on the selected winter day, Table 3 provides the DNI hourly distribution.

As far as the biomass is concerned, the thermo-chemical characteristics are typical of short rotation forestry derived woody pellet, with a lower heating value of about 17 MJ/kg and high carbon and oxygen ratios.

Table 3. Direct normal insulation data for the selected winter day [25].

Hour	DNI [kJ/h m^2]	Hour	DNI [kJ/h m^2]
1	0	13	3,377
2	0	14	3,305
3	0	15	3,053
4	0	16	2,019
5	0	17	66
6	0	18	0
7	0	19	0
8	66	20	0
9	2,019	21	0
10	3,053	22	0
11	3,305	23	0
12	3,377	24	0

4. Combined solar-biomass plant behaviour

The analysis of solar-biomass plant is based on the comparison of transient and overall performance under two power modulation scenarios. Namely, the tracking of the end-user thermal load in the hypothesis of electric energy surplus sale to the grid, and the tracking of the end-user electric load with a dump of the thermal energy surplus.

In the following, the overall CHP plant performances are first discussed on a yearly and monthly basis and then the time-dependent results on a winter day are shown and discussed. In particular, the study focuses on a typical winter day in order to discuss the behaviour of the system in operating conditions which are not favourable to the solar sub-system. The thermal and electric load curves are shown in Figure 6. The thermal load ranges from 300 to 640 kW, with a sharp min-max modulation. On the other hand, the electric load, always below 100 kW, achieves its peak level in the morning and then it decreases during the day being nearly constant in the afternoon and evening times.

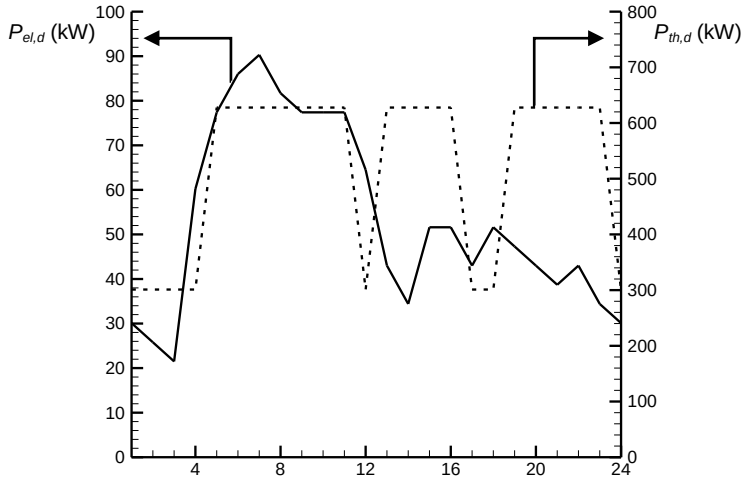

Figure 6. End user electric and thermal load for a typical winter day [23].

4.1. Overall power system performance

In order to compare the performance of the solar-biomass CHP system under the two proposed load-tracking logics, a number of indicators have been considered (Table 4). In particular the indices concern the RES system performance, the output performance and the RC efficiency. The surplus and deficit index for the output performance were calculated by adding the surplus or deficit thermal and electric energy production which occurred hour per hour with respect to the corresponding load energy request. The overall performances have been computed over a year period. CORREGGI PUNTO CON VIRGOLA PER MIGLIAIA E AL CONTRARIO PER DECIMALI

Table 4. Overall performance data.

		Electric Tracking	Thermal Tracking
RES system	Solar energy [GJ/y]	4˙277,53	4˙277,53
	Effective solar energy supply [GJ/y]	4˙172,09	4˙092,72
	Biomass energy [GJ/y]	18˙132,39	17˙221,31
	Solar fraction	18,71	19,20
	Biomass consumption [ton/y]	990,84	941,06
	Global effective energy input E_g [GJ/y]	22˙304,48	21˙314,03
Electric output	Plant electric energy output E_{el} [GJ/y]	**2˙064,37**	2˙017,10
	$E_{el,d}$ [GJ/y]	**1˙664,68**	1˙664,46
	E_{el}/ $E_{el,d}$ [%]	**124,01**	121,19
	Surplus [%]	**19,80**	25,80
	Deficit [%]	**0,44**	8,32
Thermal output	Plant thermal energy supply E_{th}[GJ/y]	17˙291,93	**16˙895,49**
	$E_{th,d}$ [GJ/y]	11˙656,13	**11˙653,99**
	E_{th}/ $E_{th,d}$ [%]	148,35	**144,98**
	Surplus [%]	40,09	**33,27**
	Deficit [%]	7,49	**2,26**
RC system	Net electric efficiency = E_{el}/E_g [%]	9,26	9,46
	Net thermal efficiency = E_{th}/E_g [%]	77,53	79,27
	Electric index = E_{el}/E_{th} [-]	11,94	11,94
	Primary energy ratio = $(E_{el}/\eta_{el}+E_{th}/\eta_{th})/E_g$ [-][1]	1,21	1,24

[1] For the primary energy ratio evaluation, the values for the reference electric and thermal efficiencies are η_{el} = 0.38 and η_{th} = 0.8.

The integration over the duty time showed that the parabolic trough field collect s 4˙277.53 GJ/y of solar energy. Furthermore, as the energy input need varies in the two scenarios in reason of the different loads, the effective solar energy supply, which is a balance between the available solar energy and the TES charge discharge rates, differs in the two cases with an amount of about 4˙172 GJ/y in the electric tracking scenario and 4˙093 GJ/y in the thermal tracking one. The biomass energy supply varies for the same reason, leading to an effective solar supply fraction, calculated as the percentage of the effective solar energy with respect to the sum of the effective solar energy and the biomass furnace energy, of 18.71% in the electric tracking case and 19.20 % in the thermal tracking one.

Looking at the RC system performance in **Errore. L'origine riferimento non è stata trovata.**, the value of 1.2 for the primary energy ratio demonstrates that the presented solar-biomass Rankine cycle systems can effectively allow the saving of conventional primary energy sources in each presented scenario. Looking at the electric output, globally the system produces more electric energy than the need with a peak production/request ratio of 124% for the electric tracking.

4.2. Overall hourly power system performance

The global data in a RES based plant are not indicative of the effective load covering. As a matter of fact, analyzing the hourly behaviour of the systems, there are both surplus and deficit situations. It is worth noting that the hospital electric tracking scenario offers a completely absence of thermal supply deficits, but shows a 132% of thermal energy surplus. Considering that the electric source is easier to manage than the thermal one, as it can be sold or bought from the grid, the most suitable configuration appears to be the thermal tracking one.

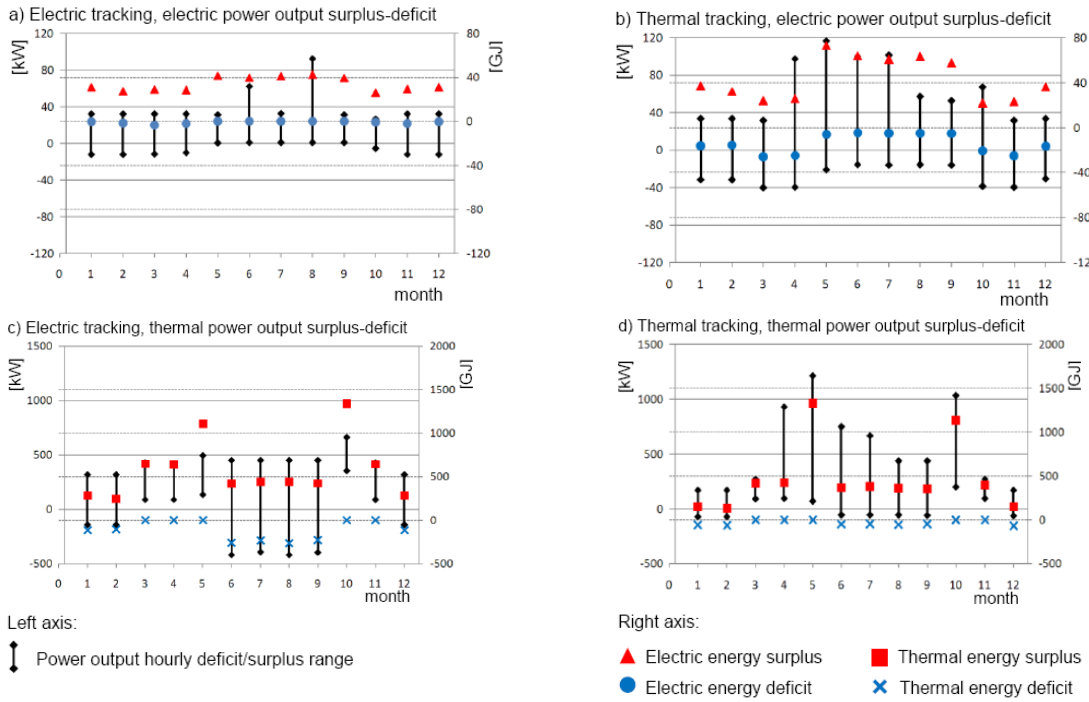

Figure 7. Hotel electric and thermal power surplus/deficit behaviour during a one year period under electric and thermal load tracking conditions.

Figure 7 shows the surplus (values higher than zero) and deficits (values lower than zero) behaviour of the electric and thermal power supply for both the electric and thermal tracking scenario. The graphs, presented on a monthly basis, are based on hourly data, and show, on the left axis, the minimum and maximum difference registered in the month between the load and the supplied power. On the right axis the cumulative surplus and deficit energy is shown for each month. Figure

7 confirms that in each case the surplus rate is higher than the deficit non è sempre vero, vedi da giugno a settembre 7.c. Moreover, the electric output of the electric tracking configuration, Figure 7 a), shows the smaller values variation. Nevertheless, as this good result corresponds to the electric behaviour on the electric tracking configuration, the thermal behaviour is worst, with a high rate of surplus distributed all over the reference year and a deficit peak during the summer period, as the electric energy request is not sufficiently high to let the system to produce the requested thermal energy too. The deficit and surplus events have a quadruple explanation. The first one is that in half the showed cases are non tracked results, e.g. when discussing the electric tracking configuration, the thermal output does not follow any production law, but is dependent from the electric production trend, without any correlation to the thermal load. Secondly, in most of the occasions the gaps with the requested load are entailed to the used correlation among load energy and hot thermal fluid flow rate, which do not perfectly fit the sensitivity analysis data, conducing to gaps between the desired output and the obtained one. Nevertheless, those gaps are not particularly remarkable. The third reason, instead, explains the high surplus peaks that occur, by observing that sometimes there are contemporarily an elevated available solar supply and full thermal energy storage. In those cases the system, which has to deliver the collected heat, sends all the hot flow rate directly to the Rankine cycle. The last reason is that the biomass furnace is always on duty, even if on a minimum rate, supplying energy also in extremely low energy request.

4.3. Matching through the thermal load tracking

The thermal load tracking case is first analysed by comparing hourly distribution of the different power components. Figure 8 shows the power inputs to the RC, respectively from the solar field (PCSP) and the biomass furnace (Pb), the TES contribution during the charge/discharge cycles (PTES,c, PTES,d), and the thermal power recovered from the exhaust gas (Peg).

As evident, the CSP power is available only between 9 a.m. and 4 p.m., with two peaks, respectively ante- and post-meridian, of about 400 kW. This means that the PCSP is not sufficient to meet the thermal load (Pth,d) which rapidly rises to its peak value about 600 kW. For this reason the control system driven by the thermal demand, activates the TES system to store fractions of the solar energy (PTES,c) available in the peak hours and to buffer it (PTES,d) in the day time when the sun DNI fall below 3,000 kJ/h m^2.

It is worth noting that the PCSP reduction at 12 a.m. is caused by the reflection losses due to multiple reflections occurring for high solar incidence angles [26]. Figure 8 demonstrates also how the control system drives the biomass heat input (Pb) by modulating it in a complementary manner with the thermal storage discharge.

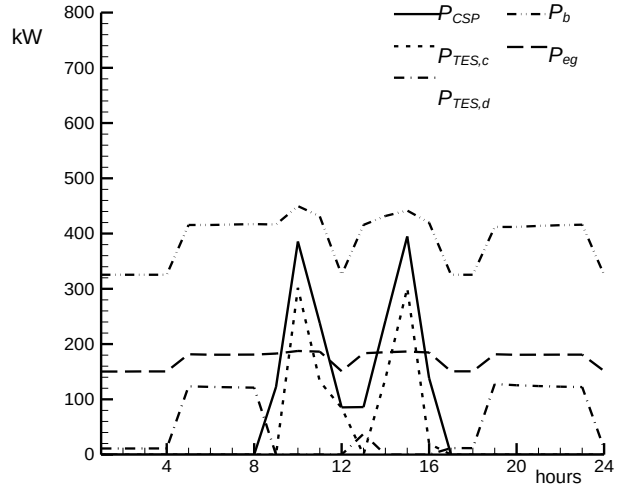

Figure 8. RES power contribution with the thermal load tracking matching.

The matching of the power plant with the end-user demand, as driven by the thermal profile, is described in Figure 9, by plotting the thermal power output (P_{th}) against the thermal power request ($P_{th,d}$) (Figure 9.a), and the electric power output (P_{el}) against the electric demand ($P_{el,d}$) (Figure 9.b). As evident in Figure 9.a, the thermal load ($P_{th,d}$) is completely satisfied by the solar-biomass plant output (P_{th}). It is worth noting that the exceeding heat production during the periods of minimum request is consequent to the control regime of the biomass furnace which is kept at a constant minimum level. When looking at the electric matching (Figure 9.b), it is remarkable that the power plant electric output (P_{el}) mimics the shape of the leading load component. As a result, the correct sizing of the solar-biomass CHP system provides a fair matching in the period of peak electric request, while the load tracking logic drives the system to an over-production of electricity during the remaining duty time.

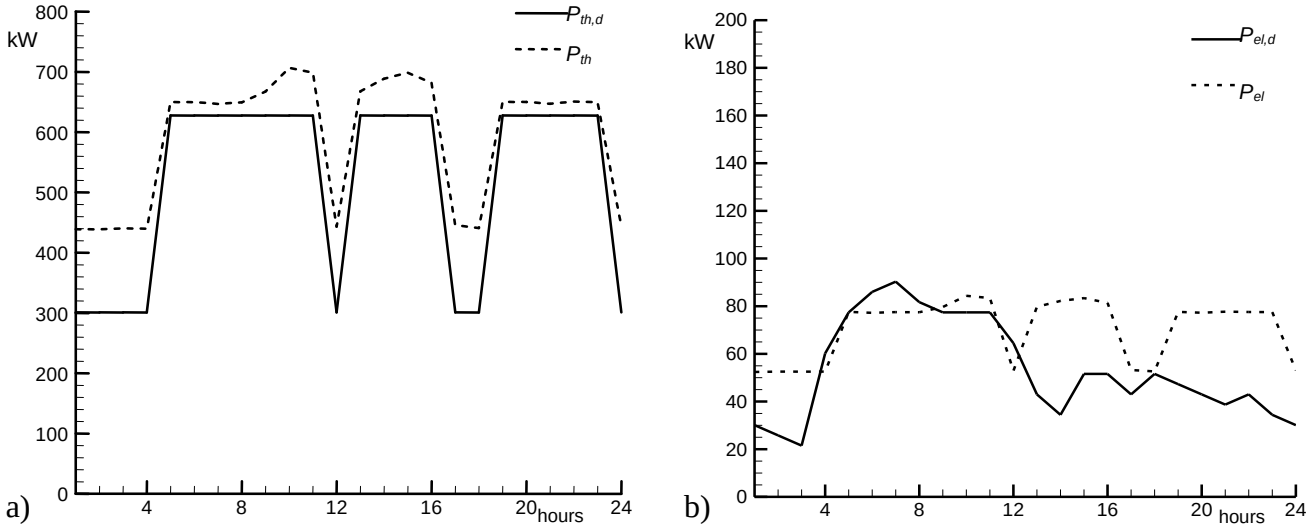

Figure 9. Thermal a) and electric b) behaviour with the thermal load tracking matching.

4.4. Matching through the electric load tracking

The analysis of solar-biomass CHP plant when matching the end-user under the electric load hypothesis is discussed in Figure 10 by comparing the different thermal power inputs to the RC system.

The modification of the load tracking logic appears to influence remarkably the RES power inputs/outputs and the TES charge/discharge cycle. In particular, while the PCSP behaviour remains linked to the DNI hourly distribution, the TES charge cycle is no more driven by solar radiation a.m. and p.m. peaks and it is shifted in the afternoon hours when the overall electric power request reduces. This circumstance causes the shifting of the TES discharge cycle to the evening time and unbalances the power input from the biomass furnace which is mainly concentrated in the early morning hours. This finding confirms that the TES and the biomass furnace have complementary behaviours by implementing an effective reserve to the solar source.

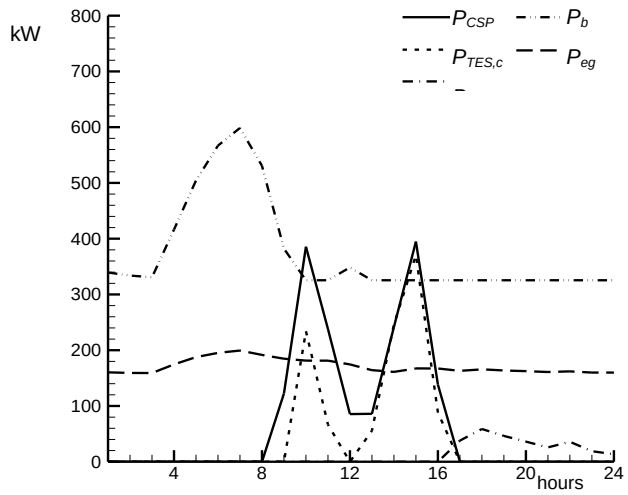

Figure 10. RES power contribution with the electric load tracking matching.

From the power output point of view, Figure 9 shows the matching of the thermal (P_{th}) (Figure 11.a) and the electric (P_{el}) (Figure 11.b) power outputs with the end-user load profiles. As a matter of fact, the thermodynamic characteristics of the solar-biomass CHP system determine the significant overproduction of the thermal power output when the overall control is given to the electricity production. As evident in Figure 11.a, the electric peak request in the early morning giving rise to the intervention of the biomass, in absence of any direct or stored solar contribution, results in a large surplus of heat availability. Moving to the electric matching, Figure 11.b, it is shown that the delivered electric power (P_{el}) follows fairly the load ($P_{el,d}$) between 4 a.m. and 12 p.m. while keeping it nearly constant in the remaining hours.

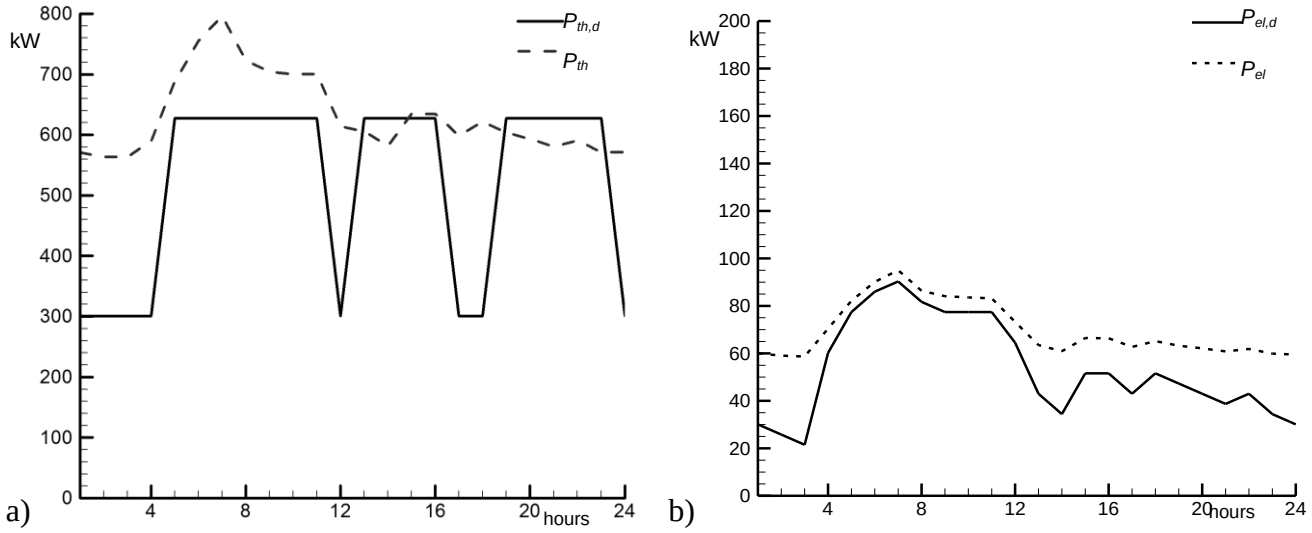

Figure 11. Thermal a) and electric b) behaviour with the electric load tracking matching.

5. Environmental and economic aspects

Although the plant potential and versatility have been analyzed, demonstrating the suitability of the plant itself to work in an off-grid configuration, referring to the electric and thermal power tracking, it is worthy to assess environmental and economic aspects also.

An effect of this system application are the entailed Greenhouse Gases (GHG) emission savings, estimated by means of emission factors related to the Italian thermoelectric power stations at reference year 2003 [23]. The emissions savings are evaluated considering the entire electric energy

supply, in the hypothesis of grid transfer of the surplus, and the fraction of thermal energy supplied to the end users, in the hypothesis of dump of the thermal energy surplus

The result is a higher emission saving in the thermal tracking scenario, which avoids the emissions of about 3˙500 ton/y of carbon dioxide.

Table 5. Global emission savings for a typical winter day.

	Electric tracking	Thermal tracking
CO_2 [ton/y]	2,967.87	3,442.71
SO_x [ton/y]	3.09	3.59
NO_x [ton/y]	1.85	2.15
TSP [ton/y]	0.12	0.14

Another essential environmental aspect is the land use of the plant. Considering the net land use, Table 6, the plant needs about 13,000 m2, nevertheless, taking into account security distances and the need of space for the power conversion block the needed surface amounts to 31,000 m2.

Table 6. Plant land use.

	Net land use
Solar field	6,780 m^2
TES	570 m^2
Biomass furnace, filter and stack	700 m^2
Biomass storage	3,000
Buildings (Rankine cycle elements, desalting units, offices)	2,100
Total	**13,150 m^2**

Concerning the plant costs, **Errore. L'origine riferimento non è stata trovata.** 7 indicates that the parabolic trough field with the thermal energy storage are the most expensive devices of the proposed system. In particular, the capital cost of a solar trough field with thermal storage has been evaluated in 4,820 $/kW for the reference year 2006 [10], that is 6,052 €/kW CIOè IL DOLLARO VALE PIù DELL'EURO?. It is worth noting that these data refer to large CSP technologies and must be considered only as a rough estimate of the present CSP device. Referring to the other technologies, the capital costs have been obtained by private communications with producers. In the utilities heading, it entails costs for electric panels, electric and hydraulic connections, civil works &c.

It is obvious that such high costs are constraining to the development of the proposed system when thinking to the standard fossil fuel based power technologies. Nevertheless, in a fossil fuel free power generation perspective, given from the exhaustion of fossil energy sources and from the need to pull down the fossil sources related emissions, the current high costs become a side issue in behalf of the sustainable development of the energy sector.

Table 7. Plant estimated capital costs.

Technology	Cost [€]
CSP field with TES	7˙870˙000
Biomass furnace	130˙000
Economizer	15˙000
Evaporator	45˙000
Steam engine	220˙000
Condenser	15˙000
Utilities	300˙000
Total	**8˙595˙000**

6. Conclusions

A model of a combined solar-biomass CHP plant devoted to feed an hotelier end-user was presented. The well-established TRNSYS software was adopted for transient simulation.

An analysis of thermal and electrical power production on a yearly bases demonstrated the feasibility of the present configuration in satisfying the energy requirements of the hotel.

Furthermore the model was matched with a thermal and an electric winter day load in transient simulations. The results for the two different load tracking scenarios were compared in terms of delivered power, matched load, RC system efficiencies and global GHG emission savings.

When looking at the output performance, the results show a most suitable behaviour for the thermal load tracking scenario, as it delivers both electric and thermal energy with less gap from the end-user requested energy. Nevertheless, the Primary Energy Ratio indicates a better behaviour for the electric load tracking.

Nomenclature

CHP	Combined Heat and Power
CSP	Concentrated Solar Power
DNI	Direct Normal Irradiation
Eel	Electric energy output
Eg	Global energy input from biomass and solar radiation
Eth	Thermal energy output
HTF	Heat Transfer Fluid
$\dot{m}_F$	HTF flow rate
$\dot{m}_{F,CSP}$	Solar field HTF delivered flow rate
$\dot{m}_{F,bmin}$	Minimum biomass furnace HTF delivered flow rate
$\dot{m}_{F,b+}$	Additional biomass furnace HTF delivered flow rate
$\dot{m}_{F,d}$	HTF demanded flow rate
$\dot{m}_{F,s}$	Solar direct and TES delivered flow rate
$\dot{m}_{F,TESc}$	TES HTF charge flow rate
$\dot{m}_{F,TESd}$	TES HTF discharge flow rate
Pb	Biomass derived power
Pb,min	Biomass furnace power at minimum duty
PCSP	CSP derived thermal power
Peg	Exhaust gas power
Pel	Electric power output
Pel,d	Electric load power
PTES,c	Storage charge power
PTES,d	Storage discharge power
Pth	Thermal power output
Pth,d	Thermal load power
RC	Rankine Cycle
RES	Renewable Energy Source
TES	Thermal Energy Storage
ηel	Reference electric efficiency
ηth	Reference thermal efficiency

References

[1] Maidment, G.G., Zhao, X., Riffat, S.B. and Prosser G., "Application of combined heat-and-power and absorption cooling in supermarkets", Applied Energy 63 (1999) 169-190.

[2] Maidment, G.G. and Tozer, R.M., "Combined cooling heat and power in supermarkets", Applied Thermal Engineering 22 (2002) 653-665.

[3] Corsini, V. Naso, G. Mattei, P. Venturini. "Biomass co-firing: analysis of the main technical problems in coal power plants". 15th European Biomass Conference, 7-11 May, Berlin, Germany.

[4] Corsini, V. Naso, G. Mattei, P. Venturini. "Biomass co-firing: estimation of fuel requirements and land needed to feed some Italian coal power plants". 15th European Biomass Conference, 7-11 May, Berlin, Germany.

[5] Eastop T.D. and Croft D.R., "Energy efficiency for engineers and technologists" (1st ed.), Longman Scientific and Technical, Halow, Essex, 1990, p. 335.

[6] Fröhlke, K. and Haidn, O.J., "Spinning reserve system based on H2/O2 combustion". Energy Conversion, S0196-8904(96)00128-8.

[7] Kélouwani, S., Agbossou, K. and Chahine R., "Model for energy conversion in renewable energy system with hydrogen storage". Journal of Power Sources 140 (2005) 392-399.

[8] Corsini, A., Rispoli, F., Gamberale, M., and Tortora, E., 2009, "Assessment of H2- and H2O-based renewable energy-buffering systems in minor islands", Renewable Energy 34 (2009) 279–288.

[9] Sinden, G. Environmental Change Institute University of Oxford, "The practicalities of developing renewable energy stand-by capacity and intermittency". Submission to The Science and Technology Select Committee of the House of Lords, 2004.

[10] Sargent & Lundy LLC Consulting Group Chicago, Illinois, Assessment of Parabolic Trough and Power Tower Solar Technology Cost and Performance Forecasts", NREL/SR-550-34440, October 2003.

[11] Jun Li, "Scaling up concentrating solar thermal technology in China", Renewable and Sustainable Energy Reviews 13 (2009) 2051-2060.

[12] Al-Soud, M.S. and Hyayshat E.S., "A 50 MW concentrating solar power plant for Jordan", Journal of Cleaner production 17 (2008) 625-635.

[13] Dong, L., Liu, H. and Riffat, S., "Development of small-scale and micro-scale biomass fuelled CHP systems. A literature review", Applied Thermal Engineering 29(2009) 2119-2126.

[14] Badami, M. and Mura, M., "Preliminary design and controlling strategy of small-scale wood waste Rankine Cycle (RC) with a reciprocating steam engine (SE)", Energy 34 (2009) 1315-1324.

[15] Borello, D., Corsini, A., Rispoli, F. and Tortora E., "A combined solar-biomass Rankine cycle concept for small-size cogeneration", Proceedings of ECOS 2009 Conference.

[16] Borello, D., Corsini, A., Rispoli, F. and Tortora E., "Load matching for a combined solar-biomass Rankine cycle plant" Proceedings of ASME-ATI-UIT 2010 Conference.

[17] Klein, S.A., Beckam, W.A., Mitchell, J.W., Braun, J.E., Evan,s B.L., Kummert J.P., et al., 2000, "TRNSYS – a transient system simulation program. Version 15.1", Madison: Solar Energy Laboratory, University of Wisconsin; 2000.

[18] Schwarzbözl, P., Eiden, U., Pitz-Paal, R., Jones, S., 2002, "A TRNSYS model library for solar thermal electric components (STEC). A reference manual." Release 2.2.

[19] Corsini, A., Gamberale, M., and Rispoli F., 2006, "Assessment of renewable energy solutions in an Italian small island energy system using a transient simulation model", ASME Journal of Solar Energy Engineering 2006;128:237–44.

[20] Jones, S.A., Pitz-Paal, R., Schwarzboezl, P., Blair, N. and Cable R., 2001, “TRNSYS modeling of the SEGS VI parabolic trough solar electric generating system”, Proceedings of Solar Forum 2001: Solar Energy: The Power to Choose, April 21-25, 2001, Washington, DC.

[21] Kolb, G.J. and Hassani, V., 2006, Performance of thermocline energy storage proposed for the 1 MW Saguaro solar trough plant, ISEC2006-99005.

[22] Siangsukone, P. and Lovegrove, K., 2002, “Modelling of a steam based paraboloidal dish concentrator using the computer source code TRNSYS”, Proceedings of Solar 2002 - Australian and New Zealand Solar Energy Society.

[23] Macchi, E., Campanari, S., Silva, P., “La micocogenerazione a gas naturale”, Polipress - Politecnico di Milano, 2005.

[24] National Action Plan for Energy Efficiency Sector Collaborative on Energy Efficiency, Hotel Energy Use Profile, EPA Summer Workshop Report, 2007.

[25] SEL, 25 July 2003, Generated Hourly Weather Data. Solar Energy Laboratory, University of Wisconsin-Madison. 12 November 2008 <http://sel.me.wisc.edu/trnsys/weather/generate.htm>.

[26] Ronnelid, M., Perers, B., Karlsson, B., “On the factorization of incidence angle modifiers for CPC collectors”, S0038-092X(97)00016-9, Solar Energy, 1997.